

Bulk and single-cell RNA sequencing identify prognostic signatures related to FGFBP2⁺ NK cell in hepatocellular carcinoma

Yinbing Wu^{1,*}, Huanjun Peng^{1,*}, Guangkang Chen¹, Yinuo Tu¹ and Xinpei Yu²

- ¹ Department of Hepatobiliary Surgery, Affiliated Cancer Hospital & Institute of Guangzhou Medical University, Guangzhou, China
- ² Department of Oncology, Affiliated Cancer Hospital & Institute of Guangzhou Medical University, Guangzhou, China

ABSTRACT

Background. Hepatocellular carcinoma (HCC) is a highly aggressive malignancy. As a specific immune cell subpopulation, FGFBP2⁺ NK cells play a crucial part in immune surveillance of HCC progression. This study set out to identify prognostic signature related to FGFBP2⁺ NK cell in HCC.

Methods. Bulk and scRNA-seq data were derived from the public databases. The single cell atlas of HCC and heterogeneity of natural killer (NK) cells were delineated by "Seurat" package. Pseudo-time trajectory of FGFBP2⁺ NK cell was constructed by "Monocle2" package. Cell-cell interactions were analyzed by "CellChat" package. Prognostic signature was screened to develop a RiskScore model, and the prediction robustness was verified. Immune cell infiltration and immunotherapy response were assessed between different risk groups. Drug sensitivity was predicted by "oncoPredict" package. The expressions of the prognosis gene signature were detected by in vitro test utilizing HCC cells. The effects of key genes on the proliferative, migratory and invasive capacity of HCC cells were assessed by EdU assay, wound healing and Transwell assay. **Results**. The proportion of NK cell in HCC samples was markedly decreased than that in healthy samples. NK cell was further divided into three cell subpopulations, and FGFBP2+ NK cell was associated with the prognosis of HCC patients. Pseudotime trajectory analysis of FGFBP2⁺ NK cell revealed two differential expression gene clusters. FGFBP2⁺ NK cell exhibited extensive intercellular communication in HCC. Further, eight prognostic signatures were identified, including six "risk" genes (UBE2F, AHSA1, PTP4A2, CDKN2D, FTL, RGS2) and two "protective" genes (KLF2, GZMH). RiskScore model was established with good prognostic prediction performance. In comparison to low-risk group, high-risk group had poorer prognosis, lower immune cell infiltration, and higher TIDE score. Moreover, 16 drugs showed significant correlation with RiskScore. Additionally, the expressions of GZMH was downregulated while FTL, PTP4A2, UBE2F, CDKN2D, RGS2, and AHSA1 were upregulated in HCC cells. FTL and PTP4A2 silencing could suppress the proliferation, migration and invasion abilities of HCC cells.

Conclusion. This study identified eight prognostic gene signatures related to FGFBP2⁺ NK cell in HCC, which may serve as potential therapeutic targets for HCC.

Submitted 7 January 2025 Accepted 27 March 2025 Published 20 May 2025

Corresponding authors Yinuo Tu, tuyinuo123@126.com Xinpei Yu, yxinpei@gzhmu.edu.cn

Academic editor Fanglin Guan

Additional Information and Declarations can be found on page 17

DOI 10.7717/peerj.19337

© Copyright 2025 Wu et al.

Distributed under Creative Commons CC-BY 4.0

OPEN ACCESS

These authors contributed equally to this work.

Subjects Bioinformatics, Cell Biology, Gastroenterology and Hepatology, Immunology, Oncology **Keywords** Hepatocellular carcinoma, FGFBP2⁺ NK cell, Prognostic signature, Tumor microenvironment, Immunotherapy, Bulk RNA sequencing, Single-cell RNA sequencing

INTRODUCTION

Hepatocellular carcinoma (HCC) accounts for 80–90% of all primary liver cancer cases (*Li*, Liu & Qin, 2022; Zhou et al., 2024) and is the fifth most frequently diagnosed malignancy and third highest in carcinoma-relevant mortality around the world (*Zhao et al.*, 2019; Li et al., 2024d; Sensi et al., 2024). It is generally believed that the critical risk factors leading to HCC primarily comprise hepatitis B/C virus infection, non-alcoholic fatty liver, and excessive alcohol consumption (Wang et al., 2021; Cao, Hu & Tang, 2023). Owing to the lack of obvious clinical symptoms and effective intervention strategies, the treatment outcomes for HCC have constantly attracted much attention (Kong & Yao, 2021). For the moment, the detection of HCC in clinical is widely dependent on the imaging approaches such as ultrasonography, computerized tomography, and magnetic resonance (Zhou et al., 2020b), as well as tumor biomarkers (particularly α -fetoprotein) (Wu et al., 2022). However, the specificity and sensitivity of these screening techniques are far from satisfactory. As a consequence, most patients with HCC have progressed into advanced stage when diagnosed (Du et al., 2021). In addition, despite chemotherapy, radiotherapy, targeted therapy, and immunotherapy have recently made remarkable progression (*Liu et al.*, 2023), the prognostic outcomes of HCC remains disappointing due to the high recurrence and metastasis rate, with the 5-year survival probability <30% (Zhu et al., 2023b). Therefore, it is essential to develop novel prognostic signatures and offer promising therapeutic targets for HCC.

Researches have manifested that the prognosis of HCC patients is usually affected by the complicated tumor microenvironment (TME) (Zhu et al., 2023a). In recent years, immunotherapy such as immune checkpoint inhibitors (ICIs) have shown great promise in the treatment of HCC (Huang et al., 2021a). Whereas, one of the main barriers to effective immunotherapy is TME, which may contribute to immune tolerance and evasion in HCC (Luo et al., 2022). Comprehensive excavation of the concealed information in TME is critical for understanding the pathogenesis of HCC and improving the patient prognosis (Wu et al., 2024). Natural killer (NK) cell belongs to a member of innate immunity and is primarily found in human liver (Shin et al., 2024). NK cell has strong cytotoxicity and immunosurveillance potential, exerting crucial roles in the first-line immune defense against HCC development (Hong et al., 2022). The dysfunction of NK cell is considered to be a vital mechanism of immune escape in HCC (Sung & Jang, 2018). It has been confirmed that compared with healthy individuals, the proportion of NK cell is markedly decreased in the patients with advanced HCC (*Hosseinzadeh et al.*, 2018). Immune cell therapy targeting NK cell has been emphatically recognized as the novel standard of care for advanced HCC (Hosseinzadeh et al., 2019). Given the important immune regulation roles of NK cell in HCC, in-depth exploration of NK cell at molecular levels is likely to facilitate the discovery of new immunotherapy strategies.

The single-cell RNA sequencing (scRNA-seq) technique can reveal the heterogeneity and dynamic changes of specific cells in TME, while bulk RNA sequencing can provide the whole transcriptomic information of tumor samples (*Chen et al.*, 2024; *Chen, Lin & Luo*, 2024). In this study, by integrating bulk and scRNA-seq analysis, we revealed the single cell atlas of HCC and the heterogeneity of NK cell. Further, we analyzed the correlation between NK cell (especially FGFBP2⁺ NK cell) with the prognostic outcomes of HCC. A prognostic gene signature was then identified to construct RiskScore model, and the immune cell infiltration, as well as immunotherapy response was assessed between different risk groups. In addition, the impacts of prognostic signatures on HCC cell proliferation, migration and invasion were assessed by *in vitro* validation tests. We hope that this study could provide novel targets for immunotherapy in HCC, thereby enhancing treatment effectiveness and improving survival rates.

MATERIAL AND METHODS

Data collection and preprocessing

RNA sequencing data and clinical follow-up data of HCC samples were downloaded from The Cancer Genome Atlas (TCGA) database through Genomic Data Commons (GDC) Application Programming Interface (API). The ICGC-LIRI-JP dataset was collected from the HCCDB database. Then, after deleting samples that did not have clinical follow-up data or status, the Ensembl was transformed to a gene symbol, and the expression average value was taken for multiple gene symbols. Finally, 370 tumor samples and 50 control samples were acquired in TCGA-LIHC cohort, utilizing as the training set. The ICGC-LIRI-JP cohort contained 212 HCC samples, which was served as the validation set.

The scRNA-seq data of GSE162616 dataset, including three HCC samples and three healthy liver samples, was derived from the Gene Expression Omnibus (GEO) database. For filtering the scRNA-seq data, each gene was set to be expressed in a minimum of three cells, and each cell expressed at least 200 genes. Then, the cells with nFeature_RNA >300, nCount_RNA >3,000, and mitochondrial gene expression percent.mito <25% were reserved. The NormalizeData function was applied for log conversion, and the FindVariableFeatures function was used to identify highly variable genes. Next, the ScaleData function was utilized to normalize the expression values of all genes, the RunPCA function was employed for principal component analysis (PCA), and the "harmony" R package was used to remove batch effects between different samples (*Zulibiya et al.*, 2023).

Cell clustering analysis

Cell clustering analysis of GSE162616 dataset was conducted using the "Seurat" R package (*Du et al.*, 2024). Firstly, UMAP was conducted on the top 15 principal components (PCs) for dimensionality reduction. Then, the cells were clustered using the FindNeighbors and FindClusters functions, with cluster resolution of 0.1 for all cells and 0.3 for NK cells. Finally, cell types were annotated based on the marker genes provided by CellMarker2.0 database (*Lu et al.*, 2024).

Single-sample gene set enrichment analysis

The correlation between the prognosis of HCC and each type of NK cells was examined based on the single-sample gene set enrichment analysis (ssGSEA) score calculated utilizing "GSVA" R package for the tumor samples in TCGA-LIHC cohort (*Wang et al.*, 2023). The surv_cutpoint function was applied to find the optimal cut-off point, and HCC patients were divided into low- and high-score groups.

Pseudo-time trajectory analysis

In order to invesitgate the role of FGFBP2⁺ NK cell in the progression of HCC, Monocle2 was used to construct pseudo-time trajectory (*Tao et al.*, 2024). The cds object was established by newCellDataSet function, and the genes expressed in less than 10 cells were filtered out. The differentially expressed genes (DEGs) between HCC samples and healthy samples were identified by differentialGeneTest function, and Kyoto Encyclopedia of Genes and Genomes (KEGG) enrichment analysis was conducted on these DEGs using the "ClusterProlifer" R package (*Zhang et al.*, 2024). Subsequently, the reduceDimension function was employed for dimensionality reduction (max_components = 2, method = "DDRTree"), and the orderCells function was applied to order the cells and construct the pseudo-time trajectory of FGFBP2⁺ NK cell.

Cellular communication analysis

The "CellChat" R package was employed to conduct cell–cell interaction analysis in HCC (*Lian et al.*, 2024). The number of interactions and interaction weights/strength was analyzed, as well as the key ligand–receptor pairs between FGFBP2⁺ NK cell and other cell subpopulations were visualized by a bubble plot.

Establishment and verification of RiskScore model

Univariate Cox regression analysis (p < 0.05) was performed on the marker genes of FGFBP2⁺ NK cell. The number of genes in the model was reduced by LASSO Cox regression analysis was conducted using the "glmnet" R package (Zeng & Chen, 2024). By 10-fold cross validation, we selected the optimal lambda value as the result of LASSO regression for subsequent analysis. Further, stepwise regression analysis was performed, and the prognostic gene signature related to FGFBP2⁺ NK cell in HCC was identified to establish RiskScore model. The RiskScore of each patient in TCGA-LIHC cohort was obtained according to the following formula ($Li \ et \ al., 2024a$):

$$RiskScore = \sum \beta i^* ExPi$$

 β is the coefficient of gene in Cox regression model, and i is the gene expression.

Z-score was utilized for standardization, and based on the threshold of RiskScore = 0, high- and low-risk groups were classified. To evaluate the prognostic prediction performance of RiskScore model, receiver operating characteristic (ROC) analysis was conducted using the "timeROC" R package (*Lin et al.*, 2023). Additionally, the robustness of RiskScore model was validated in the ICGC-LIRI-JP cohort.

Immune cell infiltration and immunotherapy response analysis

Immune cell infiltration was assessed between high- and low-risk groups in TCGA-LIHC cohort. StromalScore, ImmuneScore, and ESTIMATEScore were calculated by the "estimate" R package (*Dong et al.*, 2023). Tumor Immune Estimation Resource (TIMER) was applied to assess the infiltration of six immune cells (*Xiao et al.*, 2020). Microenvironment cell populations-counter (MCP-counter) algorithm was utilized to assess the infiltration of 10 immune cells (*Chen et al.*, 2022).

The response of different risk groups to immunotherapy was predicted by TIDE algorithm (*Li et al.*, 2024b). Exclusion, Dysfunction, and TIDE scores of different risk groups were calculated in TCGA-LIHC cohort. Moreover, we analyzed the relationship of RiskScore and 9 immune checkpoint genes.

Correlation analysis between RiskScore and drug sensitivity

The IC₅₀ values of drugs for HCC patients in TCGA-LIHC cohort were predicted using the "oncoPredict" R package (*Maeser*, *Gruener & Huang*, 2021). Then, the association between RiskScore and drug sensitivity was analyzed (p < 0.05 and |cor| > 0.3).

Cell culture and transfection

Human hepatic astrocyte cell line LX-2 (BNCC337957) and HCC cell line Huh7 (BNCC337690) were acquired from the BeNa Culture Collection (BNCC) Biotechnology Co. (Beijing, China). Then, LX-2 and Huh7 cell lines were separately cultivated in RPMI-1640 (BNCC338360) and DMEM (BNCC363314) contained 10% fetal bovine serum (FBS), and were all incubated in the condition of 5% CO₂ and 37 °C. Hereafter, according to the protocol of Lipofectamine 2000 (Invitrogen, Waltham, MA, USA), Huh7 cells were transfected with the small interfering (si) RNA of *FTL* (si-*FTL*: 5′-TCCCAGATTCGTCAGAATTATTC-3′, Sangon, China), (si) RNA of *PTP4A2* (si-*PTP4A2*: 5′-GAGGTTCTATGTGCCATAATTAA-3′, Sangon, China) and negative control (si-NC). We have performed short tandem repeat (STR) identification on the cells, and the mycoplasma detection results turned out to be negative.

Quantitative real-time PCR

Total RNA of LX-2 and Huh7 cells were acquired employing the Trizol reagent (B610409, Sangon, China). Then, the complementary DNA (cDNA) was synthesized through reverse transcription applying the RevertAid First Strand cDNA Synthesis Kit (B300538, Sangon, China). Thereafter, quantitative real-time PCR (qRT-PCR) amplification was performed using the SYBR Green (B110031, Sangon, China) on the basis of manufacturer's instructions. The qPCR conditions were: 94 °C for 30 s first, then 40 cycles of 94 °C for 5 s and 60 °C for 30 s. The primer pairs of this study were shown in Table S1. *GAPDH* was utilized as an internal control to normalize the relative mRNA expressions of each gene by $2^{-\Delta\Delta CT}$ method (*Xu et al.*, 2020b).

Proliferation assay

Huh-7 cells that had been transfected were maintained for 48 h until they reached the logarithmic growth phase, after which they were moved into 96-well plates. The EdU

Cell Proliferation Assay Kit (RiboBio, Guangzhou, China) was utilized to evaluate cell proliferation. In accordance with the established protocol, the cells underwent staining, followed by examination and imaging using a fluorescence microscope (Nikon, Toyko, Japan). EdU-positive cell counts were conducted using ImageJ software.

Wound healing assay

The effect of FTL and PTP4A2 silencing on the migration of HCC cells Huh7 was measured by wound healing assay (*Song et al.*, 2021). The transfected Huh7 cells (1×10^5) were inoculated into a 6-well plate and grown overnight. Afterwards, the wound was created using a sterile 20 μ L pipette tip and Huh7 cells were sustainably cultured in serum-free medium for 48 h. Finally, the pictures of wound areas at 0 hour (h) and 48 h were obtained under a microscope (ECLIPSE Ei, Nikon, Tokyo, Japan), and the wound closure (%) of Huh7 cells was estimated with the ImageJ2 software.

Transwell assay

Transwell assay was conducted to examine the influence of FTL and PTP4A2 silencing on the invasion of HCC cells Huh7 ($Huang\ et\ al.,\ 2021b$). The diluted Matrigel (BD Biosciences, Franklin Lakes, NJ, USA) was pre-coated into the Transwell chamber (8.0 μ m, Corning, Corning, NY, USA). Next, the transfected Huh7 cells (1 \times 10⁵) were starved in the upper chamber encompassing 200 μ L non-serum medium. 500 μ L DMEM containing 10% FBS was filled into the lower chamber. After 48 h of incubation, the invaded Huh7 cells were fixed by 4% paraformaldehyde (YTB1299, bjbalb, Beijing, China) and dyed by 0.1% crystal violet (YT913, bjbalb, Beijing, China). Further, the number of invaded Huh7 cells was counted under the same microscope as above.

Statistical analysis

The bioinformatic analysis was conducted using R programing language (version 4.1.0). The differences between different groups were compared by the Wilcoxon rank-sum test. Kaplan–Meier (K-M) analysis of overall survival (OS) was conducted by log-rank test. The Spearman method was utilized for correlation analysis. All experimental data of independent triplicates were expressed as mean \pm standard deviation,, and statistical analysis was carried out by GraphPad Prism8.0. For data that did not conform to a normal distribution, non-parametric tests such as the Mann–Whitney U test or Kruskal-Wallis test were applied. p < 0.05 signified statistical significance.

RESULTS

Single-cell atlas of HCC revealed the reduction proportion of NK cell

The scRNA-seq data of GSE162616 dataset was analyzed to delineate the single-cell atlas of HCC. After cell filtration, standardization, dimensionality reduction, and clustering, a total of 47,550 cells were obtained and divided into 11 cell clusters (Fig. S1). Using the marker genes, these cells were further annotated as seven cell types (Fig. 1A), comprising NK cell (GZMB, GZMH, FGFBP2, GNLY, CD160), T cell (CD2, CD3D, CD3E, IL7R), macrophage (AIF1, MS4A7, LYZ), plasma cell (DERL3, IGHG1, MZB1), CD8⁺ T cell (MKI67, STMN1),

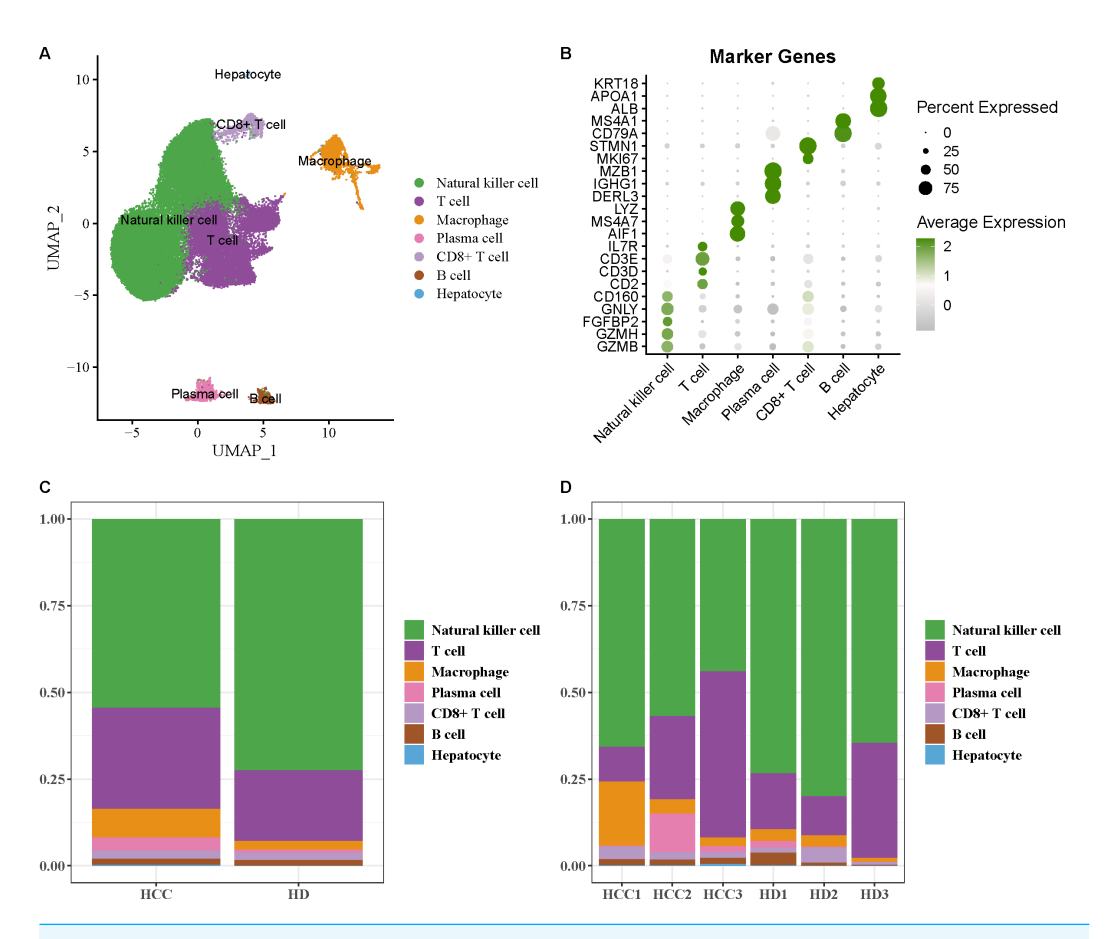


Figure 1 Single-cell atlas of hepatocellular carcinoma (HCC). (A) UMAP plot of cell subpopulations after annotation; (B) Expression level of marker genes in each cell type; (C–D) Proportion of each cell type in different samples.

B cell (*CD79A*, *MS4A1*), and hepatocyte (*ALB*, *APOA1*, *KRT18*) (Fig. 1B). Additionally, the proportion of each cell type in different samples was analyzed, showing that the number of NK cell in HCC samples was markedly decreased compared with healthy samples (Figs. 1C and 1D). These results indicated that the proliferation and activity of NK cell may be inhibited in HCC microenvironment.

FGFBP2⁺ NK cell was associated with the prognosis of HCC patients

NK cell as an important immune cell can recognize and kill tumor cells. Hence, we extracted the NK cell from HCC tissues for re-clustering, obtaining three cell subpopulations (Fig. 2A). The top20 highly expressed genes in each NK cell subpopulation were displayed by a heatmap (Fig. 2B). Using the marker genes, these cell subpopulations were annotated as FGFBP2⁺ NK cell (*FGFBP2*, *FCGR3A*, *GZMB*, *GZMH*), CD160⁺ NK cell (*GZMK*, *CD160*), and IL7R⁺ NK cell (*IL7R*, *SELL*, *LMNA*, *CD44*) (Fig. 2C). Compared with healthy samples, the proportion of FGFBP2⁺ NK cell and IL7R⁺ NK cell was elevated while CD160⁺ NK cell was decreased in HCC samples (Fig. 2D). Furthermore, K-M survival curve suggested that FGFBP2⁺ NK cell exhibited an association with the prognosis of HCC patients (p = 0.047),

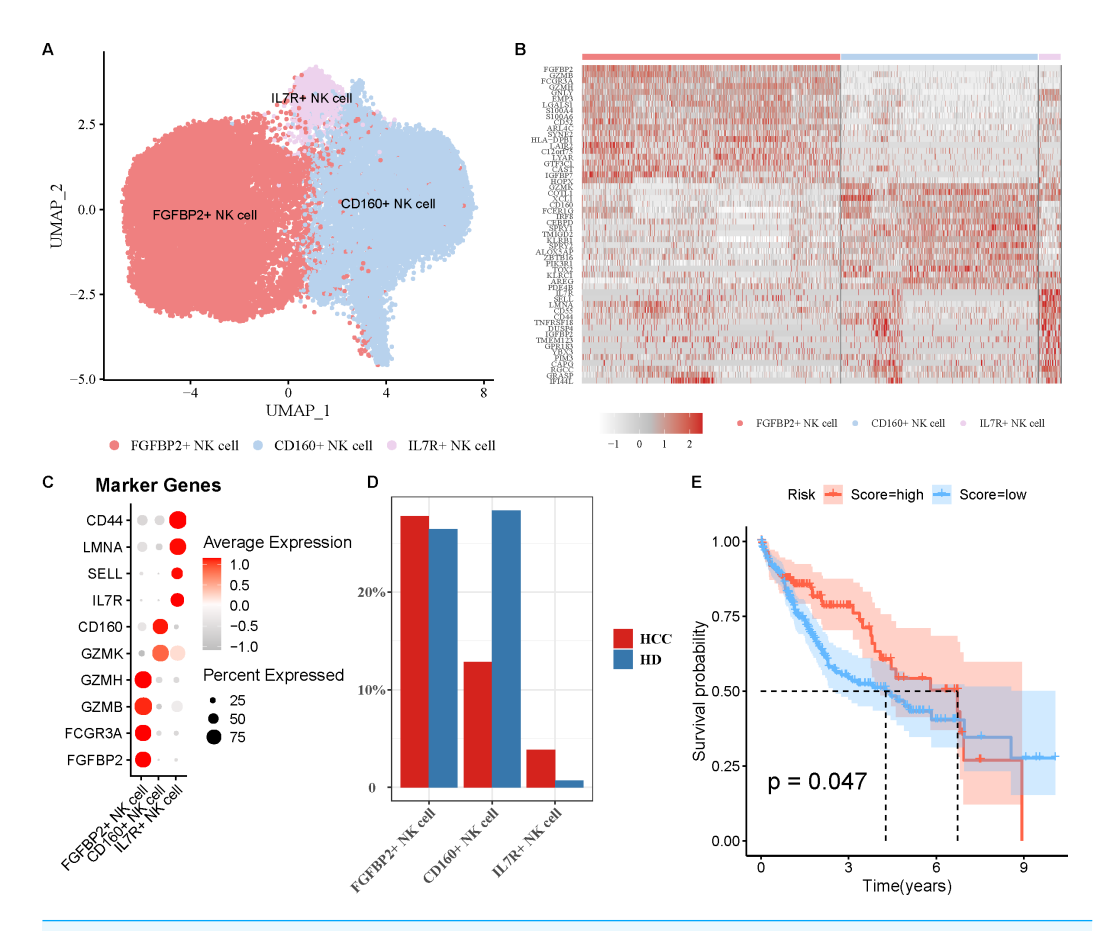


Figure 2 Analysis of natural killer (NK) cell heterogeneity. (A) UMAP plot of NK cell subpopulations after annotation; (B) Highly expressed genes in each NK cell type; (C) Marker genes in each NK cell type; (D) Proportion of each NK cell type in different samples; (E) Kaplan–Meier (K–M) survival curve of ss-GSEA score of FGFBP2⁺ NK cell in TCGA-LIHC cohort.

with higher survival probability in high ssGSEA score group in comparison to the low ssGSEA score group (Fig. 2E). Whereas, CD160⁺ NK cell (p = 0.082) and IL7R⁺ NK cell (p = 0.1) was not closely related to the prognosis of HCC patients (Fig. S2).

Pseudo-time trajectory of FGFBP2⁺ NK cell from normal to HCC was constructed

For further exploring the role of FGFBP2⁺ NK cell in HCC progression, the pseudo-time trajectory of FGFBP2⁺ NK cell from normal to HCC was constructed by Monocle2, and the branch with more healthy samples was set as the starting point, and the branch with more HCC samples was set as the ending point (Figs. 3A and 3B). Moreover, DEGs analysis between HCC samples and healthy samples revealed two differential expression gene clusters, and the gene expression in Cluster1 was gradually up-regulated with the increase of pseudo-time (Fig. 3C). KEGG enrichment analysis demonstrated that the DEGs in Cluster1 were primarily involved in the endocytosis, protein processing in nuclear factor (NF)-kappa B signaling pathway, endoplasmic reticulum, apoptosis, antigen processing and presentation, NK cell mediated cytotoxicity (Fig. 3D). These pathways might play a

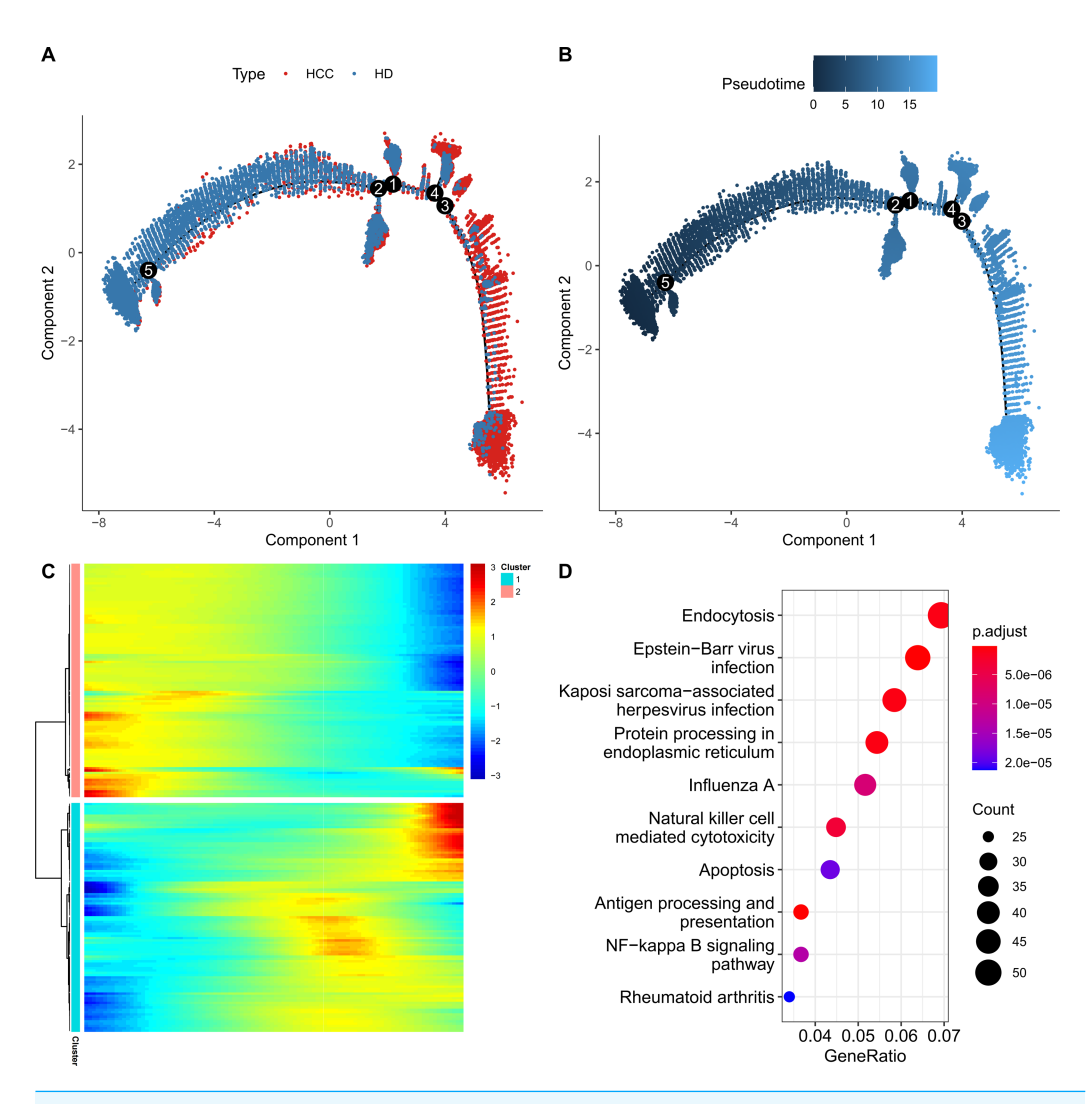


Figure 3 Construction of pseudo-time trajectory of FGFBP2⁺ NK cell. (A–B) Differentiation trajectory of FGFBP2⁺ NK cell from normal to HCC; (C) Heatmap of DEGs between HCC samples and healthy samples; (D) KEGG enrichment pathways of DEGs in Cluster1.

crucial role in the process of FGFBP2⁺ NK cells transitioning from the normal state to be involved in HCC.

FGFBP2⁺ NK cell exhibited extensive intercellular communication in HCC

Cellular communication analysis was performed to explore the potential interactions between different cell types in HCC. It was observed that the number and strength of ligand–receptor interactions was complicated (Fig. 4A). FGFBP2⁺ NK cell as signal sender showed extensive communication with Macrophage, B cell, IL7R⁺ NK cell, T cell, CD160⁺ NK cell, and CD8⁺ T cell (Fig. 4B). By extracting the critical ligand–receptor pairs, we found that FGFBP2⁺ NK cell communicated with other cell subpopulations *via* tumor

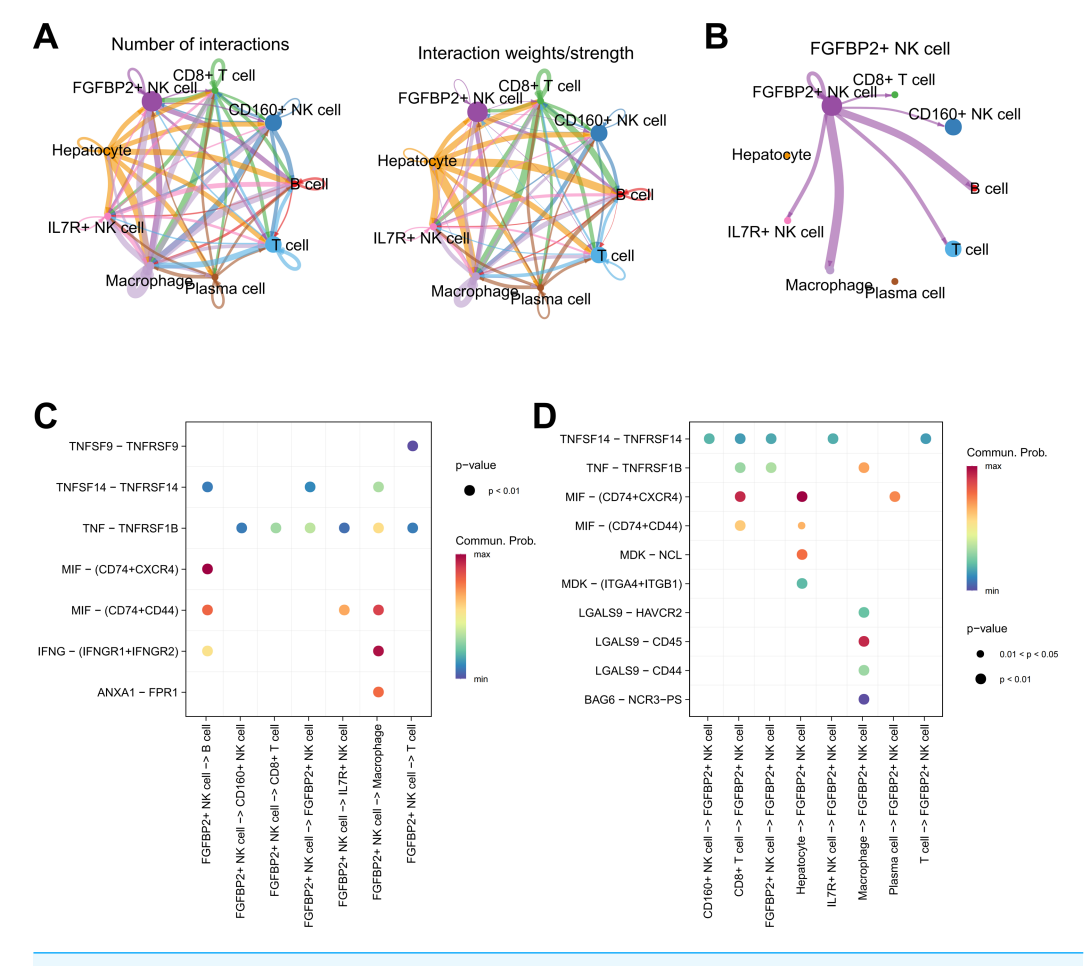


Figure 4 Cellular communication analysis in HCC. (A) Cell–cell interactions network between different cell subpopulations; (B) Cell communication of FGFBP2⁺ NK cell as a signal sender; (C) Key ligand–receptor pairs of FGFBP2⁺ NK cell acting on other cell subpopulations; (D) Key ligand–receptor pairs of other cell subpopulations acting on FGFBP2⁺ NK cell.

necrosis factor (TNF)-TNFRSF1B and macrophage migration inhibitory factor (MIF)-(CD74+CD44) (Fig. 4C), while other cell subpopulations communicated with FGFBP2⁺ NK cell *via* TNFSF14-TNFRSF14 and MIF-(CD74+CXCR4) (Fig. 4D).

RiskScore model was constructed and verified based on 8-genes prognostic signature

Firstly, the marker genes in FGFBP2⁺ NK cell were subjected to univariate Cox regression analysis (p < 0.05). LASSO and stepwise regression analysis was further performed to reduce the gene number, and the model was optimal when the lambda was 0.0286 (Figs. 5A and 5B). Then, eight prognostic signatures related to FGFBP2⁺ NK cell in HCC were identified, including six "risk" genes (UBE2F, AHSA1, PTP4A2, CDKN2D, FTL, RGS2) and two "protective" genes (KLF2, GZMH) (Fig. 5C). Next, we established a RiskScore model of "RiskScore = -0.352*GZMH-0.303*KLF2+0.153*FTL+0.312*PTP4A2+0.442*UBE2F+0.234*CDKN2D+0.141*RGS2+0.427*AHSA1".

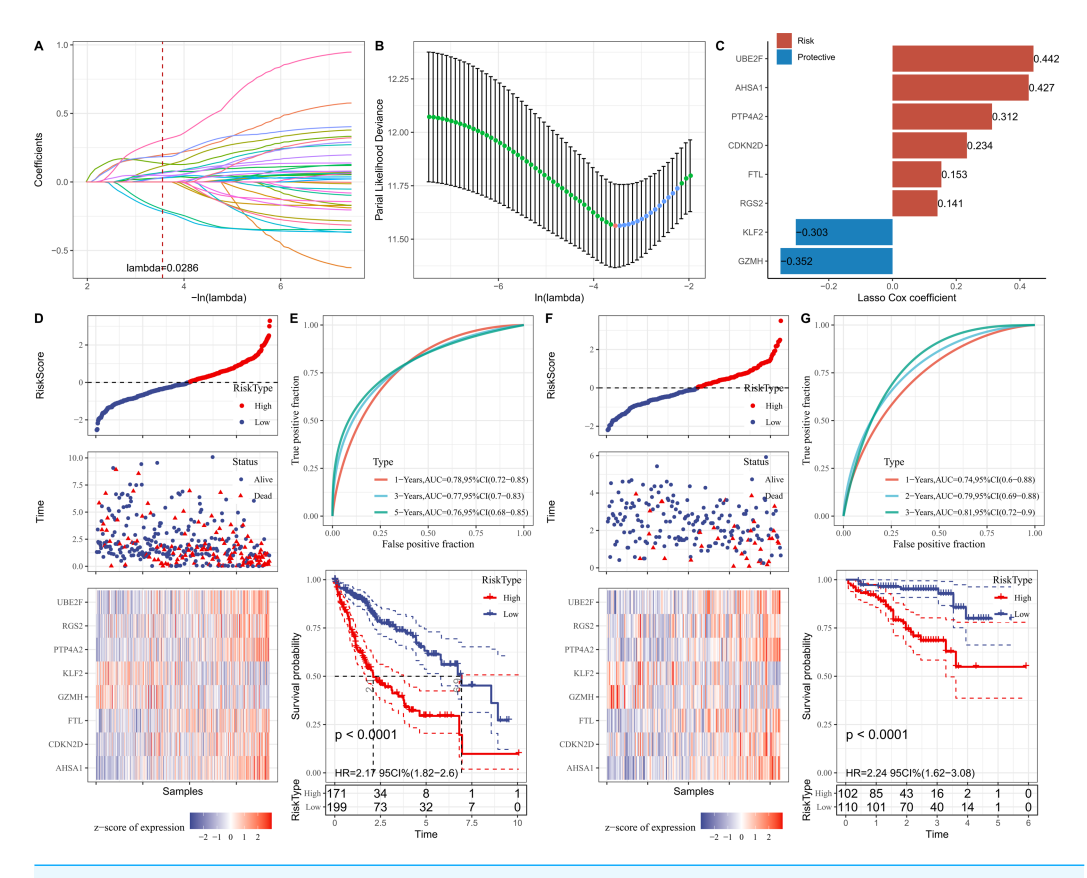


Figure 5 Establishment and verification of RiskScore model. (A) Coefficients of each independent variable; (B) Confidence interval for each lambda; (C) Prognostic gene signatures in RiskScore model; (D) RiskScore, survival status, and signature expression level in TCGA-LIHC cohort; (E) ROC analysis and K-M survival curves in TCGA-LIHC cohort; (F) RiskScore, survival Status, and signature expression level in ICGC-LIRI-JP cohort; (G) ROC analysis and K-M survival curves in ICGC-LIRI-JP cohort.

Furthermore, according to the threshold of RiskScore = 0, all samples in TCGA-LIHC cohort were separated into high- and low-risk groups (Fig. 5D). The performance of RiskScore model was evaluated by the area under ROC curve (AUC). It was showed that 1-, 3-, 5-years AUC values of the RiskScore model were 0.78, 0.77, 0.76 (Fig. 5E), which manifested that the RiskScore model exhibited good prognostic prediction performance. K-M curve analysis suggested that the OS rate of high-risk group was lower (Fig. 5E), showing that HCC patients with high RiskScore may have a poor prognosis. The robustness of RiskScore model was verified in ICGC-LIRI-JP cohort, and the results of which were similar to the TCGA-LIHC cohort (Figs. 5F and 5G). These outcomes demonstrated the reliability of the RiskScore model in the prognostic predicting of HCC.

RiskScore model exhibited potential in predicting immunotherapy response for HCC

We first elucidated the association between RiskScore and immune cell infiltration. ESTIMATE algorithm results showed that compared to low-risk group, high-risk group had lower StromalScore, ImmuneScore, and ESTIMATEScore (Fig. 6A). Based on the

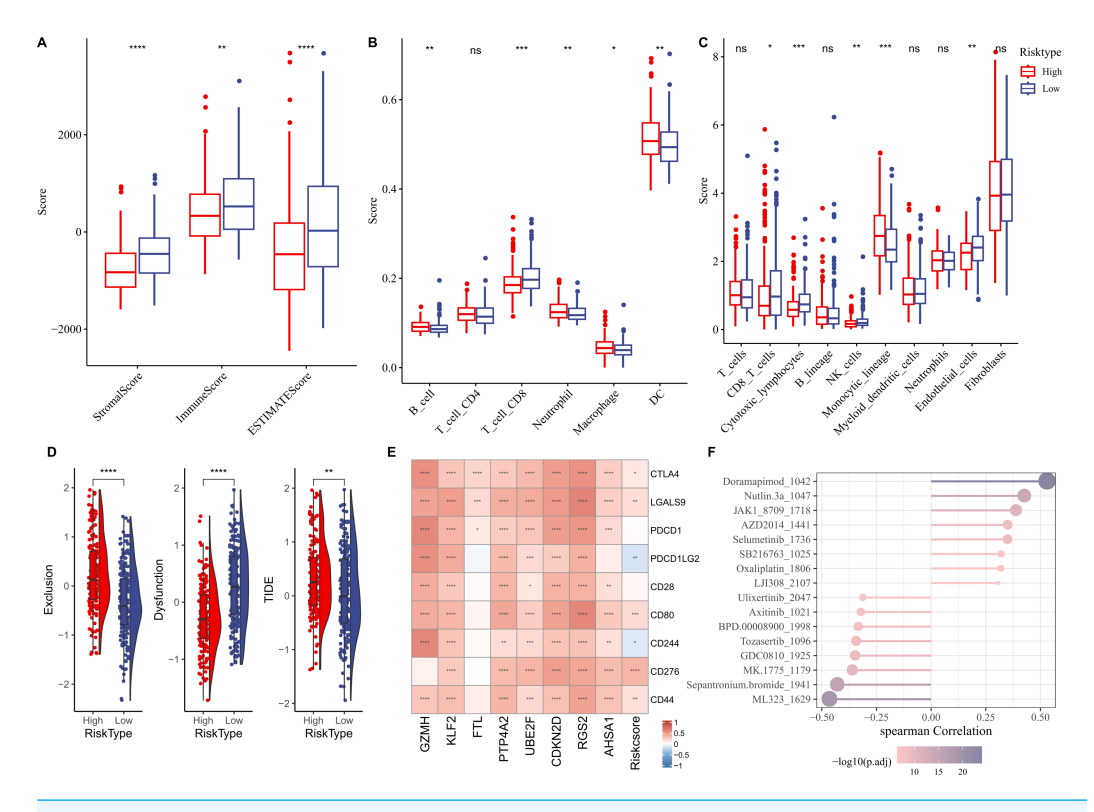


Figure 6 Correlation analysis between immune cell infiltration, immunotherapy response and RiskScore. (A) StromalScore, ImmuneScore, and ESTIMATEScore between different risk groups; (B) Infiltration levels of six immune cells assessed by TIMER website; (C) Infiltration levels of 10 immune cells calculated by MCP-counter algorithm; (D) Exclusion, Dysfunction, and TIDE scores in different risk groups; (E) Relationship between RiskScore and immune checkpoint genes; (F) Correlation between RiskScore and drugs IC50; **** indicates p < 0.001; ** indicates p < 0.001; * indicates p < 0.05; ns indicates not significant.

TIMER database, the infiltration levels of neutrophil, B cell, macrophage, and dendritic cell (DC) in high-risk group were significantly higher, while CD8 T cell was notably lower in comparison to the low-risk group (Fig. 6B). MCP-counter algorithm suggested that the infiltration levels of CD8 T cell, cytotoxic lymphocytes, NK cell, and endothelial cell were markedly lower, yet monocytic lineage was higher in high-risk group (Fig. 6C). In addition, the immunotherapy response between different risk groups was predicted in TCGA-LIHC cohort. In comparison to low-risk group, high-risk group exhibited higher exclusion score and TIDE score (Fig. 6D), demonstrating that high-risk HCC patients may be less likely to benefit from taking immunotherapy. RiskScore was positively correlated with several immune checkpoint genes, including *CD44*, *CD276*, *CD80*, *LGALS9*, and *CTLA4* (Fig. 6E), showing that HCC patients with higher RiskScore may be more possibly to experience immune escape. Furthermore, we examined the association between drug sensitivity and RiskScore, and screened 16 drugs (such as Doramapimod, Nutlin.3a, Selumetinib, Sepantronium bromide, Tozasertib) that showed significant correlation with RiskScore (p < 0.05 and |cor| > 0.3) (Fig. 6F).

In vitro HCC cell-based model to validate key genes

The qRT-PCR analysis demonstrated that in comparison to the human hepatic astrocyte cells LX-2, the relative mRNA expression levels of *GZMH* was remarkably lower, yet *FTL*, *PTP4A2*, *UBE2F*, *CDKN2D*, *RGS2*, and *AHSA1* were notably higher in HCC cells Huh7 (Fig. 7A). Since the pro-carcinogenic role of *FTL* in HCC has been reported in related studies, and the functional mechanism of *PTP4A2* in HCC lacks systematic studies, we chose these two genes for *in vitro* functional experiments to further validate their roles in HCC cell migration, invasion and proliferation. Thereafter, we verified the knockdown efficiency of these two genes in Huh-7 cells (Fig. S3). We observed a significant decrease in proliferation of HCC cell lines after silencing *FTL* and *PTP4A2* (Fig. 7B). In addition, wound healing assay displayed that *FTL* and *PTP4A2* silencing could decrease the wound closure rate of Huh7 cells (Fig. 7C). Transwell assay suggested that the number of invading Huh7 cells was reduced by the silencing of *FTL* and *PTP4A2* (Fig. 7D). Consequently, these results indicated the crucial involvement of *FTL* and *PTP4A2* in HCC progression.

DISCUSSION

Numerous studies have indicated that NK cell function crucially in the surveillance and control of HCC, and NK cell dysfunction or exhaustion is implicated in the pathogenesis of advanced HCC (*Eresen et al.*, 2024; *Lee et al.*, 2021b). The prognostic significance of NK cell in TME of HCC has been widely concerned, and NK cell is highly considered as a promising target for tumor immunotherapy (*Yang et al.*, 2023; *Li et al.*, 2023). In this study, we innovatively combined scRNA-seq and bulk RNA-seq analyses to systematically resolve the heterogeneity of FGFBP2⁺ NK cells in HCC and its association with prognosis, and constructed a RiskScore model based on FGFBP2⁺ NK cell-related genes, which provides a new molecular basis for prognostic assessment of HCC patients and immunotherapy response prediction. Compared with previous studies, this study not only revealed the role of FGFBP2⁺ NK cells in the HCC microenvironment, but also explored the function of their related genes in HCC progression, revealing new potential targets for NK cell-targeted immunotherapy.

FGFBP2 served as the signature gene responsible for the cytotoxic killing function within NK cells (*Li et al.*, 2010). Some researchers have identified FGFBP2 as a key gene involved in NK cell-mediated immune response in ankylosing spondylitis (*Chen et al.*, 2025). Cui et al. (2024) identified two cell subpopulations in NK cells of HCC, including FGFBP2⁺ NK cells and B3GNT7⁺ NK cells. They suggested that the impairment of these functional anticancer cells is the potential cause of HCC. These studies suggest that the reduction of FGFBP2⁺ NK cells may impair the cytotoxic activity of NK cells, which in turn affects the immune response and prognosis of HCC patients, suggesting that it is expected to be a potential target for HCC immunotherapy. In addition, the eight prognostic signatures related to FGFBP2⁺ NK cell in HCC comprised six "risk" genes (*UBE2F*, AHSA1, PTP4A2, CDKN2D, FTL, and RGS2) and two "protective" genes (*KLF2*, and GZMH). In vitro assays showed that compared with the human hepatic astrocyte cells LX-2, the relative mRNA expressions of FTL, PTP4A2, UBE2F, CDKN2D, RGS2, and AHSA1 were notably higher

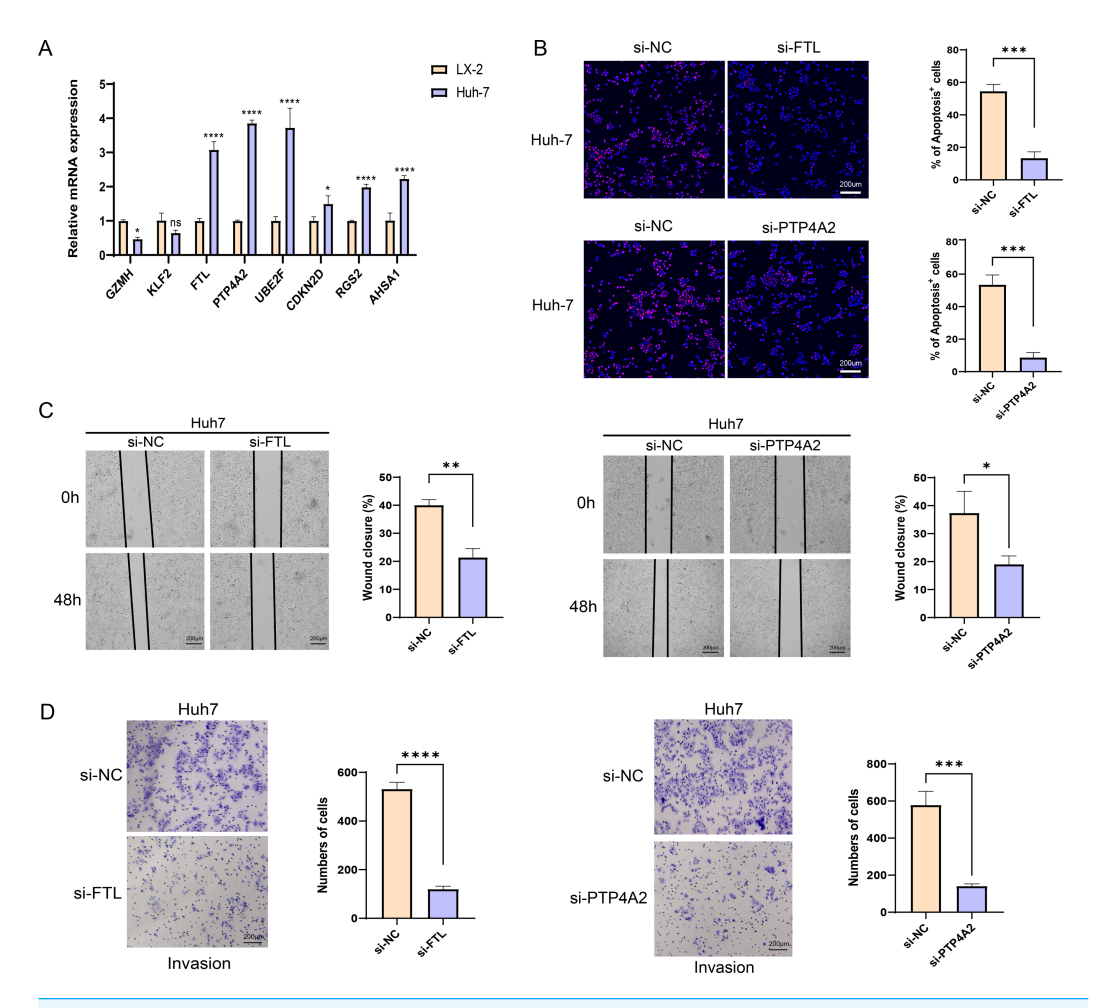


Figure 7 Effects of *FTL* and *PTP4A2* silencing on the migration and invasion abilities of HCC cells. (A) Relative mRNA expression of eight prognostic gene signatures detected by qRT-PCR; (B) Effect of *FTL* and *PTP4A2* silencing on the proliferation ability of HCC cells was evaluated by EdU assay; (C) Impact of *FTL* and *PTP4A2* silencing on the migration capability of HCC cells assessed *via* Wound healing assay; (D) Effect of *FTL* and *PTP4A2* silencing on the invasion ability of HCC cells evaluated *via* Transwell assay; **** denotes p < 0.0001; *** denotes p < 0.001; ** denotes p < 0.05.

Full-size DOI: 10.7717/peerj.19337/fig-7

in HCC cells Huh7. *UBE2F*, a ubiquitin-conjugating enzyme, is usually over-expressed in many malignant tumors such as lung cancer, resulting in a low OS rate (*Zhou et al.*, 2020a). Targeting *UBE2F* might serve as an effective sensitizing strategy of chemo-/radiotherapy through triggering tumor cell apoptosis (*Zhou et al.*, 2023). *AHSA1*, principally implicated in the activity of ATPase activators, is observed the upregulation of *AHSA1* in HCC that is linked to clinical stage and worse outcomes of patients (*Gao et al.*, 2023). Cell-based assays have manifested that knockdown of *AHSA1* can inhibit the proliferation, migration, and invasion capabilities of HCC cells (*Li & Liu*, 2022). *PTP4A2* belongs to a member of regenerating liver phosphatase family and can mediate cellular bioenergetics (*Hardy et al.*, 2023). *PTP4A2* is essential for vascular morphogenesis and angiogenesis (*Poulet et al.*, 2020), which has been deemed as a carcinogenic factor in majority of human cancers,

such as nasopharyngeal carcinoma (Gao et al., 2017) and glioblastoma (Chouleur et al., 2024). CDKN2D, a cyclin-dependent kinase inhibitor, exerts crucial roles in regulating tumor growth (Zhu et al., 2021). The abnormal expression of CDKN2D contributes to the uncontrolled proliferation of malignant cells including HCC (Lee et al., 2021a). FTL, also known as ferritin light chain, has been recognized to be one of the regulators in early iron metabolism (Kuang et al., 2023). Recent study of Ke et al. (2022) demonstrated that FTL was closely relevant to HCC progression, and patients with low FTL expression had a remarkable survival advantage. Our current study indicated that FTL silencing could markedly restrain the migration and invasion capabilities of HCC cells. RGS2, belonging to a GTPase-activating protein, functions as a key regulator of G-protein signaling (Cacan, 2017). Abnormal expression of RGS2 in different tumor types is significantly correlated with poor prognosis (*Ihlow et al.*, 2022). There are few reports of RGS2 in HCC, deserving further exploration. KLF2, a transcription factor of Krüppel-like factor family, can impede the tumor cell movement mediated by TGF-β signaling in HCC (Li et al., 2020). Lin et al. (2019) observed that the expression of KLF2 was markedly decreased in HCC tissues than in adjacent tissues. GZMH, i.e., Granzyme H, exerts crucial roles in tumor killing mediated by T cell and NK cell, acting as a predictor for tumor immunotherapy (*Li et al.*, 2024c). High GZMH expression is indicative of a better prognosis in HCC (Jin et al., 2024). Overall, these findings supported that the RiskScore model, constructed with eight prognostic signatures in this study, was reliable in the prognostic evaluation for patients with HCC. Meanwhile, these eight prognostic signatures may be regarded as promising therapeutic targets for HCC.

Furthermore, we found that the ImmuneScore in high-risk group was remarkably lower than that in low-risk group. The infiltration levels of B cell, neutrophil, macrophage, and monocytic lineage were observably higher while CD8 T cell, cytotoxic lymphocytes, NK cell, and endothelial cell were markedly lower in high-risk group than low-risk group. CD8 T cell plays an anti-tumor effect through releasing interferon-γ and TNF cytokines (Huo, Wu & Zang, 2021). Cytotoxic T lymphocytes exert crucial roles in anti-tumor immunity by recognizing and eliminating cancer cells (Akazawa et al., 2019). NK cell has strong anti-tumor activity via producing cytotoxic and cytokine (Zecca et al., 2020). This suggested that the infiltration characteristics of immune cells form an immunosuppressive microenvironment that may be closely correlated with a worse prognosis of HCC patients (Sun et al., 2023). The immunotherapy response in different risk groups was further predicted by TIDE algorithm, and high-risk group showed a higher TIDE score than low-risk HCC patients, which indicated that HCC patients in high-risk group might benefit limitedly from ICIs treatment (Liu et al., 2022). Moreover, the RiskScore exhibited positive correlation with several immune checkpoint genes, including CD44, CD276, CD80, LGALS9, and CTLA4, demonstrating that HCC patients with higher RiskScore may be more possibly to experience immune evasion (*Xu et al.*, 2020a). Hence, these immune checkpoint genes could be the targets for HCC immunotherapy. In addition, the correlation between RiskScore and drug sensitivity was analyzed, and 16 drugs (such as Doramapimod, Nutlin.3a, Selumetinib, Sepantronium bromide, and Tozasertib) were screened, which supplied some reference for drug selection of HCC patients.

Nevertheless, there are also some shortcomings of the current study. The RiskScore model was constructed based on eight gene signatures, which was identified entirely from the data of public databases. It is necessary to further validate with prospective clinical data. Moreover, the specific mechanism of the eight prognostic gene signatures in HCC has not yet been investigated. In the future, we will consider performing a large number of *in vivo* and *in vitro* experiments to verify our outcomes.

CONCLUSION

In summary, based on bulk and scRNA-seq analysis, this study revealed eight prognostic gene signatures related to FGFBP2⁺ NK cell in HCC, which were utilized to create a RiskScore model. This model exhibited strong performance in assessing the prognostic outcomes and immunotherapy of HCC patients. 16 drugs were screened to be correlated with RiskScore. Additionally, *FTL* and *PTP4A2* expression was upregulated in HCC cells, and their silencing significantly inhibited cell proliferation, migration, and invasive capacity. This study could provide promising therapeutic targets for HCC patients and also supply some reference for drug development.

Abbreviations

API Application Programming Interface

AUC area under ROC curve
BNCC BeNa Culture Collection
cDNA complementary DNA

DC dendritic cell

DEGs differentially expressed genes

FBS fetal bovine serum

GDC Genomic Data Commons
GEO Gene Expression Omnibus
HCC hepatocellular carcinoma

IC50 half maximal inhibitory concentration

ICIs immune checkpoint inhibitors

KEGG Kyoto Encyclopedia of Genes and Genomes

K-M Kaplan–Meier

LASSO least absolute shrinkage and selection operator
MCP-counter microenvironment cell populations-counter
MIF Macrophage migration inhibitory factor

NF nuclear factor NK Natural killer OS overall survival

PCA principal component analysis

qRT-PCR quantitative real-time polymerase chain reaction

ROC receiver operating characteristic scRNA-seq single-cell RNA sequencing

si small interfering

ssGSEA single-sample gene set enrichment analysis

TCGA The Cancer Genome Atlas

TIDE Tumor Immunity Dysfunction and Exclusion

TIMER Tumor Immune Estimation Resource

TME tumor microenvironment TNF tumor necrosis factor

UMAP uniform manifold approximation and projection

ADDITIONAL INFORMATION AND DECLARATIONS

Funding

This study was supported by Science popularization special project of Department of Science and Technology of Guangdong Province (2023A1414020055). The funders had no role in study design, data collection and analysis, decision to publish, or preparation of the manuscript.

Grant Disclosures

The following grant information was disclosed by the authors:

Science popularization special project of Department of Science and Technology of Guangdong Province: 2023A1414020055.

Competing Interests

The authors declare there are no competing interests.

Author Contributions

- Yinbing Wu conceived and designed the experiments, performed the experiments, analyzed the data, prepared figures and/or tables, authored or reviewed drafts of the article, and approved the final draft.
- Huanjun Peng conceived and designed the experiments, prepared figures and/or tables, and approved the final draft.
- Guangkang Chen performed the experiments, analyzed the data, authored or reviewed drafts of the article, and approved the final draft.
- Yinuo Tu performed the experiments, prepared figures and/or tables, and approved the final draft.
- Xinpei Yu conceived and designed the experiments, analyzed the data, authored or reviewed drafts of the article, and approved the final draft.

Data Availability

The following information was supplied regarding data availability:

The datasets generated and/or analyzed during the current study are available at GEO: GSE162616.

The raw data is available in Github and Zenodo:

- https://github.com/yinuotu356/All-raw-data.git
- yinuotu356. (2025). yinuotu356/All-raw-data: Updated raw data (v.1.1.1). Zenodo. https://doi.org/10.5281/zenodo.14986495.

Supplemental Information

Supplemental information for this article can be found online at http://dx.doi.org/10.7717/peerj.19337#supplemental-information.

REFERENCES

- Akazawa Y, Nobuoka D, Takahashi M, Yoshikawa T, Shimomura M, Mizuno S, Fujiwara T, Nakamoto Y, Nakatsura T. 2019. Higher human lymphocyte antigen class I expression in early-stage cancer cells leads to high sensitivity for cytotoxic T lymphocytes. *Cancer Science* 110(6):1842–1852 DOI 10.1111/cas.14022.
- Cacan E. 2017. Epigenetic regulation of RGS2 (Regulator of G-protein signaling 2) in chemoresistant ovarian cancer cells. *Journal of Chemotherapy (Florence, Italy)* 29(3):173–178 DOI 10.1080/1120009X.2016.1277007.
- Cao Y, Hu L, Tang Y. 2023. Hepatitis B virus X protein-mediated upregulation of miR-221 activates the CXCL12-CXCR4 axis to promote NKT cells in HBV-related hepatocellular carcinoma. *Biocell* 47(7):1537–1548 DOI 10.32604/biocell.2023.027205.
- Chen Y, Li Y, Xu Y, Lv Q, Ye Y, Gu J. 2025. Revealing the role of natural killer cells in ankylosing spondylitis: identifying diagnostic biomarkers and therapeutic targets. *Annals of Medicine* 57(1):2457523 DOI 10.1080/07853890.2025.2457523.
- Chen J, Lin A, Luo P. 2024. Advancing pharmaceutical research: a comprehensive review of cutting-edge tools and technologies. *Current Pharmaceutical Analysis* 21(1):1–19 DOI 10.1016/j.cpan.2024.11.001.
- Chen C, Wang S, Tang Y, Liu H, Tu D, Su B, Peng R, Jin S, Jiang G, Cao J, Zhang C, Bai D. 2024. Identifying epithelial-mesenchymal transition-related genes as prognostic biomarkers and therapeutic targets of hepatocellular carcinoma by integrated analysis of single-cell and bulk-RNA sequencing data. *Translational Cancer Research* 13(8):4257–4277 DOI 10.21037/tcr-24-521.
- Chen H, Zhang Z, Zhou L, Cai T, Liu B, Wang L, Yang J. 2022. Identification of CCL19 as a novel immune-related biomarker in diabetic nephropathy. *Frontiers in Genetics* 13:830437 DOI 10.3389/fgene.2022.830437.
- Chouleur T, Emanuelli A, Souleyreau W, Derieppe MA, Leboucq T, Hardy S, Mathivet T, Tremblay ML, Bikfalvi A. 2024. PTP4A2 promotes glioblastoma progression and macrophage polarization under microenvironmental pressure. *Cancer Research Communications* 4(7):1702–1714 DOI 10.1158/2767-9764.CRC-23-0334.
- Cui Z, Li H, Liu C, Wang J, Chen C, Hu S, Zhao X, Li G. 2024. Single-cell data revealed exhaustion of characteristic NK cell subpopulations and T cell subpopulations in hepatocellular carcinoma. *Aging* 16(7):6550–6565 DOI 10.18632/aging.205723.
- **Dong B, Cheng R, Zeng H, Chen L, Zhou L. 2023.** Identification and validation of co-expressed immune-related gene signature affecting the pattern of immune infiltrating in esophageal cancer. *Combinatorial Chemistry & High Throughput Screening* **26(4)**:756–768 DOI 10.2174/1386207325666220705105906.
- **Du Y, Jiang X, Zhang Y, Ying J, Yi Q. 2024.** Integrating single-cell and bulk RNA-seq to construct a metastasis-related model for evaluating immunotherapy and

- chemotherapy in uveal melanoma. *Current Medicinal Chemistry* **31(42)**:7030–7042 DOI 10.2174/0109298673286355231222054226.
- **Du Y, Ma X, Wang D, Wang Y, Zhang T, Bai L, Liu Y, Chen S. 2021.** Identification of heterogeneous nuclear ribonucleoprotein as a candidate biomarker for diagnosis and prognosis of hepatocellular carcinoma. *Journal of Gastrointestinal Oncology* **12(5)**:2361–2376 DOI 10.21037/jgo-21-468.
- Eresen A, Pang Y, Zhang Z, Hou Q, Chen Z, Yu G, Wang Y, Yaghmai V, Zhang Z. 2024. Sorafenib plus memory like natural killer cell combination therapy in hepatocellular carcinoma. *American Journal of Cancer Research* 14(1):344–354 DOI 10.62347/PMVN1173.
- Gao Y, Li Y, Liu Z, Dong Y, Yang S, Wu B, Xiao M, Chen C, Wen Y, Chen L, Jiang H, Yao Y. 2023. AHSA1 regulates hepatocellular carcinoma progression via the TGF-β/Akt-Cyclin D1/CDK6 pathway. *Journal of Hepatocellular Carcinoma* 10:2021–2036 DOI 10.2147/JHC.S407680.
- Gao Y, Zhang M, Zheng Z, He Y, Zhu Y, Cheng Q, Rong J, Weng H, Chen C, Xu Y, Yun M, Zhang J, Ye S. 2017. Over-expression of protein tyrosine phosphatase 4A2 correlates with tumor progression and poor prognosis in nasopharyngeal carcinoma. *Oncotarget* 8(44):77527–77539 DOI 10.18632/oncotarget.20550.
- Hardy S, Zolotarov Y, Coleman J, Roitman S, Khursheed H, Aubry I, Uetani N, Tremblay ML. 2023. PRL-1/2 phosphatases control TRPM7 magnesium-dependent function to regulate cellular bioenergetics. *Proceedings of the National Academy of Sciences of the United States of America* 120(14):e2221083120 DOI 10.1073/pnas.2221083120.
- **Hong G, Xie S, Guo Z, Zhang D, Ge S, Zhang S, Gao W. 2022.** Progression-free survival of a patient with advanced hepatocellular carcinoma treated with adoptive cell therapy using natural killer cells: a case report. *OncoTargets and Therapy* **15**:255–266 DOI 10.2147/OTT.S344707.
- Hosseinzadeh F, Ai J, Ebrahimi-Barough S, Seyhoun I, Hajifathali A, Muhammadnejad S, Hosseinzadeh F, Shadnoush M, Dabiri Oskouei F, Verdi J. 2019. Natural killer cell expansion with autologous feeder layer and anti-CD3 antibody for immune cell therapy of hepatocellular carcinoma. *Asian Pacific Journal of Cancer Prevention* 20(12):3797–3803 DOI 10.31557/APJCP.2019.20.12.3797.
- Hosseinzadeh F, Verdi J, Ai J, Hajighasemlou S, Seyhoun I, Parvizpour F, Hosseinzadeh F, Iranikhah A, Shirian S. 2018. Combinational immune-cell therapy of natural killer cells and sorafenib for advanced hepatocellular carcinoma: a review. *Cancer Cell International* 18:133 DOI 10.1186/s12935-018-0624-x.
- Huang Y, Huang X, Zeng J, Lin J. 2021b. Knockdown of MUC16 (CA125) enhances the migration and invasion of hepatocellular carcinoma cells. *Frontiers in Oncology* 11:667669 DOI 10.3389/fonc.2021.667669.
- Huang C, Zhang C, Sheng J, Wang D, Zhao Y, Qian L, Xie L, Meng Z. 2021a. Identification and validation of a tumor microenvironment-related gene signature in hepatocellular carcinoma prognosis. *Frontiers in Genetics* 12:717319 DOI 10.3389/fgene.2021.717319.

- **Huo J, Wu L, Zang Y. 2021.** Identification and validation of a novel immune-related signature associated with macrophages and CD8 T cell infiltration predicting overall survival for hepatocellular carcinoma. *BMC Medical Genomics* **14**(1):232 DOI 10.1186/s12920-021-01081-z.
- Ihlow J, Monjé N, Hoffmann I, Bischoff P, Sinn BV, Schmitt WD, Kunze CA, Darb-Esfahani S, Kulbe H, Braicu EI, Sehouli J, Denkert C, Horst D, Taube ET. 2022. Low expression of RGS2 promotes poor prognosis in high-grade serous ovarian cancer. *Cancer* 14(19):4620 DOI 10.3390/cancers14194620.
- **Jin Y, Dai Y, Qiao O, Hu P, Han J. 2024.** miR-1972 inhibits hepatocellular carcinoma proliferation by targeting GZMH-mediated DNA replication in the cell cycle. *The Journal of Pharmacy and Pharmacology* **77**:142–152 DOI 10.1093/jpp/rgae037.
- **Ke S, Wang C, Su Z, Lin S, Wu G. 2022.** Integrated analysis reveals critical ferroptosis regulators and FTL contribute to cancer progression in hepatocellular carcinoma. *Frontiers in Genetics* **13**:897683 DOI 10.3389/fgene.2022.897683.
- **Kong DG, Yao FZ. 2021.** CDC6 is a possible biomarker for hepatocellular carcinoma. *International Journal of Clinical and Experimental Pathology* **14**(7):811–818.
- **Kuang T, Zhang L, Chai D, Chen C, Wang W. 2023.** Construction of a T-cell exhaustion-related gene signature for predicting prognosis and immune response in hepatocellular carcinoma. *Aging* **15(12)**:5751–5774 DOI 10.18632/aging.204830.
- **Lee HA, Chu KB, Moon EK, Quan FS. 2021a.** Histone deacetylase inhibitor-induced CDKN2B and CDKN2D contribute to G2/M cell cycle arrest incurred by oxidative stress in hepatocellular carcinoma cells via forkhead box M1 suppression. *Journal of Cancer* **12(17)**:5086–5098 DOI 10.7150/jca.60027.
- Lee HA, Goh HG, Lee YS, Jung YK, Kim JH, Yim HJ, Lee MG, An H, Jeen YT, Yeon JE, Byun KS, Seo YS. 2021b. Natural killer cell activity is a risk factor for the recurrence risk after curative treatment of hepatocellular carcinoma. *BMC Gastroenterology* 21(1):258 DOI 10.1186/s12876-021-01833-2.
- Li Q, Chu Y, Yao Y, Song Q. 2024a. A Treg-related riskscore model may improve the prognosis evaluation of colorectal cancer. *The Journal of Gene Medicine* 26(2):e3668 DOI 10.1002/jgm.3668.
- Li M, Huang J, Zhan G, Li Y, Fang C, Xiang B. 2023. The novel-natural-killer-cell-related gene signature predicts the prognosis and immune status of patients with hepatocellular carcinoma. *International Journal of Molecular Sciences* 24(11):9587 DOI 10.3390/ijms24119587.
- Li X, Lei J, Shi Y, Peng Z, Gong M, Shu X. 2024b. Developing a RiskScore model based on angiogenesis-related lncRNAs for colon adenocarcinoma prognostic prediction. *Current Medicinal Chemistry* 31(17):2449–2466

 DOI 10.2174/0109298673277243231108071620.
- Li W, Liu J. 2022. The prognostic and immunotherapeutic significance of AHSA1 in pancancer, and its relationship with the proliferation and metastasis of hepatocellular carcinoma. *Frontiers in Immunology* 13:845585 DOI 10.3389/fimmu.2022.845585.
- Li K, Liu J, Qin X. 2022. Research progress of gut microbiota in hepatocellular carcinoma. *Journal of Clinical Laboratory Analysis* 36(7):e24512 DOI 10.1002/jcla.24512.

- Li X, Qu X, Li S, Lin K, Yao N, Wang N, Shi Y. 2024c. Development of a novel CD8(+) T cell-associated signature for prognostic assessment in hepatocellular carcinoma. *Cancer Control* 31:10732748241270583 DOI 10.1177/10732748241270583.
- Li J, Sze DM, Brown RD, Cowley MJ, Kaplan W, Mo SL, Yang S, Aklilu E, Kabani K, Loh YS, Yamagishi T, Chen Y, Ho PJ, Joshua DE. 2010. Clonal expansions of cytotoxic T cells exist in the blood of patients with Waldenstrom macroglobulinemia but exhibit anergic properties and are eliminated by nucleoside analogue therapy. *Blood* 115(17):3580–3588 DOI 10.1182/blood-2009-10-246991.
- Li Y, Tu S, Zeng Y, Zhang C, Deng T, Luo W, Lian L, Chen L, Xiong X, Yan X. 2020. KLF2 inhibits TGF-β-mediated cancer cell motility in hepatocellular carcinoma. *Acta Biochimica Et Biophysica Sinica* 52(5):485–494 DOI 10.1093/abbs/gmaa024.
- Li Y-N, Xiu Y-H, Tang Y-J, Cao J-L, Hou W-S, Wang A-Q, Li T-Z, Jin C-H. 2024d. Sciadopitysin exerts anticancer effects on HepG2 hepatocellular carcinoma cells by regulating reactive oxygen species-mediated signaling pathways. *Biocell* 48(7):1055–1069 DOI 10.32604/biocell.2024.050515.
- **Lian W, Xiang P, Ye C, Xiong J. 2024.** Single-cell RNA sequencing analysis reveals the role of cancerassociated fibroblasts in skin melanoma. *Current Medicinal Chemistry* **31(42)**:7015–7029 DOI 10.2174/0109298673282799231211113347.
- Lin Z, He Y, Wu Z, Yuan Y, Li X, Luo W. 2023. Comprehensive analysis of coppermetabolism-related genes about prognosis and immune microenvironment in osteosarcoma. *Scientific Reports* 13(1):15059 DOI 10.1038/s41598-023-42053-w.
- Lin J, Tan H, Nie Y, Wu D, Zheng W, Lin W, Zhu Z, Yang B, Chen X, Chen T. 2019. Krüppel-like factor 2 inhibits hepatocarcinogenesis through negative regulation of the Hedgehog pathway. *Cancer Science* 110(4):1220–1231 DOI 10.1111/cas.13961.
- Liu X, Lei X, Huang S, Yang X. 2023. Current perspectives of immunotherapy for hepatocellular carcinoma. *Combinatorial Chemistry & High Throughput Screening* 28:185–201 DOI 10.2174/0113862073255266231025111125.
- Liu Z, Qi Y, Wang H, Zhang Q, Wu Z, Wu W. 2022. Risk model of hepatocellular carcinoma based on cuproptosis-related genes. *Frontiers in Genetics* 13:1000652 DOI 10.3389/fgene.2022.1000652.
- Lu H, Xu Z, Shao L, Li P, Xia Y. 2024. High infiltration of immune cells with lower immune activity mediated the heterogeneity of gastric adenocarcinoma and promoted metastasis. *Heliyon* 10(17):e37092 DOI 10.1016/j.heliyon.2024.e37092.
- **Luo D, Liao S, Liu Y, Lin Y, Li Y, Liao X. 2022.** Holliday cross-recognition protein HJURP: association with the tumor microenvironment in hepatocellular carcinoma and with patient prognosis. *Pathology Oncology Research: POR* **28**:1610506 DOI 10.3389/pore.2022.1610506.
- Maeser D, Gruener RF, Huang RS. 2021. oncoPredict: an R package for predicting in vivo or cancer patient drug response and biomarkers from cell line screening data. *Briefings in Bioinformatics* 22(6):bbab260 DOI 10.1093/bib/bbab260.
- Poulet M, Sirois J, Boyé K, Uetani N, Hardy S, Daubon T, Dubrac A, Tremblay ML, Bikfalvi A. 2020. PRL-2 phosphatase is required for vascular morphogenesis and angiogenic signaling. *Communications Biology* 3(1):603 DOI 10.1038/s42003-020-01343-z.

- Sensi B, Angelico R, Toti L, Conte LE, Coppola A, Tisone G, Manzia TM. 2024. Mechanism, potential, and concerns of immunotherapy for hepatocellular carcinoma and liver transplantation. *Current Molecular Pharmacology* 17:e18761429310703 DOI 10.2174/0118761429310703240823045808.
- Shin SK, Oh S, Chun SK, Ahn MJ, Lee SM, Kim K, Kang H, Lee J, Shin SP, Lee J, Jung YK. 2024. Immune signature and therapeutic approach of natural killer cell in chronic liver disease and hepatocellular carcinoma. *Journal of Gastroenterology and Hepatology* 39(9):1717–1727 DOI 10.1111/jgh.16584.
- **Song F, Zhang Y, Pan Z, Zhang Q, Lu X, Huang P. 2021.** Resveratrol inhibits the migration, invasion and epithelial-mesenchymal transition in liver cancer cells through up-MiR-186-5p expression. *Zhejiang Da Xue Xue Bao. Yi Xue Ban = Journal of Zhejiang University. Medical Sciences* **50**(5):582–590 DOI 10.3724/zdxbyxb-2021-0197.
- Sun L, Liu Z, Wu Z, Ning K, Hu J, Chen Z, Wu Z, Yin X. 2023. Molecular subtype identification and signature construction based on Golgi apparatus-related genes for better prediction prognosis and immunotherapy response in hepatocellular carcinoma. *Frontiers in Immunology* 14:1113455 DOI 10.3389/fimmu.2023.1113455.
- **Sung PS, Jang JW. 2018.** Natural killer cell dysfunction in hepatocellular carcinoma: pathogenesis and clinical implications. *International Journal of Molecular Sciences* **19(11)**:3648 DOI 10.3390/ijms19113648.
- **Tao L, Jiang W, Li H, Wang X, Tian Z, Yang K, Zhu Y. 2024.** Single-cell RNA sequencing reveals that an imbalance in monocyte subsets rather than changes in gene expression patterns is a feature of postmenopausal osteoporosis. *Journal of Bone and Mineral Research* **39**(7):980–993 DOI 10.1093/jbmr/zjae065.
- Wang H, Wang H, Cui W, Zhang Q, Li J, Zhang Q. 2021. Enhanced expression of miR-889 forecasts an unfavorable prognosis and facilitates cell progression in hepatocellular carcinoma. *Diagnostic Pathology* **16(1)**:51 DOI 10.1186/s13000-021-01111-5.
- Wang X, Yu J, Wen H, Yan J, Peng K, Zhou H. 2023. Antioxidative stress protein SRXN1 can be used as a radiotherapy prognostic marker for prostate cancer. *BMC Urology* 23(1):148 DOI 10.1186/s12894-023-01319-1.
- Wu Y, Chen J, Zhu R, Huang G, Zeng J, Yu H, He Z, Han C. 2024. Integrating TCGA and single-cell sequencing data for hepatocellular carcinoma: a novel glycosylation (GLY)/tumor microenvironment (TME) classifier to predict prognosis and immunotherapy response. *Metabolites* 14(1):51 DOI 10.3390/metabo14010051.
- Wu X, Wan R, Ren L, Yang Y, Ding Y, Wang W. 2022. Circulating MicroRNA panel as a diagnostic marker for hepatocellular carcinoma. *The Turkish Journal of Gastroenterology* 33(10):844–851 DOI 10.5152/tjg.2022.21183.
- Xiao Z, Hu L, Yang L, Wang S, Gao Y, Zhu Q, Yang G, Huang D, Xu Q. 2020. TGFβ2 is a prognostic-related biomarker and correlated with immune infiltrates in gastric cancer. *Journal of Cellular and Molecular Medicine* 24(13):7151–7162 DOI 10.1111/jcmm.15164.
- Xu D, Liu X, Wang Y, Zhou K, Wu J, Chen JC, Chen C, Chen L, Zheng J. 2020a.

 Identification of immune subtypes and prognosis of hepatocellular carcinoma based

- on immune checkpoint gene expression profile. *Biomedicine & Pharmacotherapy* = *Biomedecine & Pharmacotherapie* **126**:109903 DOI 10.1016/j.biopha.2020.109903.
- Xu J, Yan B, Zhang L, Zhou L, Zhang J, Yu W, Dong X, Yao L, Shan L. 2020b. Theabrownin induces apoptosis and tumor inhibition of hepatocellular carcinoma Huh7 cells through ASK1-JNK-c-Jun pathway. *OncoTargets and Therapy* 13:8977–8987 DOI 10.2147/OTT.S254693.
- Yang Y, She S, Ren L, Zhao B, Chen D, Chen H. 2023. Prognosis and therapeutic benefits prediction based on NK cell marker genes through single-cell RNA-seq with integrated bulk RNA-seq analysis for hepatocellular carcinoma. *Frontiers in Oncology* 13:1208165 DOI 10.3389/fonc.2023.1208165.
- Zecca A, Barili V, Canetti D, Regina V, Olivani A, Carone C, Capizzuto V, Zerbato B, Trenti T, Valle RDalla, Ferrari C, Cariani E, Missale G. 2020. Energy metabolism and cell motility defect in NK-cells from patients with hepatocellular carcinoma. *Cancer Immunology, Immunotherapy: CII* 69(8):1589–1603 DOI 10.1007/s00262-020-02561-4.
- **Zeng L, Chen Z. 2024.** Screening of genes characteristic of pancreatic cancer by LASSO regression combined with support vector machine and recursive feature elimination, and immune correlation analysis. *The Journal of International Medical Research* **52(3)**:3000605241233160 DOI 10.1177/03000605241233160.
- **Zhang Y, Zhang Y, Pan C, Wang W, Yu Y. 2024.** HPV-driven heterogeneity in cervical cancer: study on the role of epithelial cells and myofibroblasts in the tumor progression based on single-cell RNA sequencing analysis. *PeerJ* 12:e18158 DOI 10.7717/peerj.18158.
- Zhao Y, You S, Yu YQ, Zhang S, Li PT, Ye YH, Zhao WX, Li J, Li Q, Jiao H, Chi XQ, Wang XM. 2019. Decreased nuclear expression of FTO in human primary hepatocellular carcinoma is associated with poor prognosis. *International Journal of Clinical and Experimental Pathology* 12(9):3376–3383.
- Zhou Y, Gu J, Yu H, Chen F, Long C, Maihemuti M, Chen T, Zhang W. 2024. Screening and identification of ESR1 as a target of icaritin in hepatocellular carcinoma: evidence from bibliometrics and bioinformatic analysis. *Current Molecular Pharmacology* 17. Epub ahead of print 18 April 2025

 DOI 10.2174/0118761429260902230925044009.
- Zhou L, Lin X, Zhu J, Zhang L, Chen S, Yang H, Jia L, Chen B. 2023. NEDD8-conjugating enzyme E2s: critical targets for cancer therapy. *Cell Death Discovery* 9:23 DOI 10.1038/s41420-023-01337-w.
- Zhou PC, Sun LQ, Shao L, Yi LZ, Li N, Fan XG. 2020b. Establishment of a pattern recognition metabolomics model for the diagnosis of hepatocellular carcinoma. *World Journal of Gastroenterology* 26(31):4607–4623 DOI 10.3748/wjg.v26.i31.4607.
- Zhou L, Zhu J, Chen W, Jiang Y, Hu T, Wang Y, Ye X, Zhan M, Ji C, Xu Z, Wang X, Gu Y, Jia L. 2020a. Induction of NEDD8-conjugating enzyme E2 UBE2F by platinum protects lung cancer cells from apoptosis and confers to platinum-insensitivity. *Cell Death & Disease* 11(11):975 DOI 10.1038/s41419-020-03184-4.

- Zhu HY, Gao YJ, Wang Y, Liang C, Zhang ZX, Chen Y. 2021. LncRNA CRNDE promotes the progression and angiogenesis of pancreatic cancer via miR-451a/CDKN2D axis. *Translational Oncology* 14(7):101088 DOI 10.1016/j.tranon.2021.101088.
- Zhu P, Pei Y, Yu J, Ding W, Yang Y, Liu F, Liu L, Huang J, Yuan S, Wang Z, Gu F, Pan Z, Chen J, Qiu J, Liu H. 2023b. High-throughput sequencing approach for the identification of lncRNA biomarkers in hepatocellular carcinoma and revealing the effect of ZFAS1/miR-150-5p on hepatocellular carcinoma progression. *PeerJ* 11:e14891 DOI 10.7717/peerj.14891.
- Zhu J, Xu X, Jiang M, Yang F, Mei Y, Zhang X. 2023a. Comprehensive characterization of ferroptosis in hepatocellular carcinoma revealing the association with prognosis and tumor immune microenvironment. *Frontiers in Oncology* **13**:1145380 DOI 10.3389/fonc.2023.1145380.
- **Zulibiya A, Wen J, Yu H, Chen X, Xu L, Ma X, Zhang B. 2023.** Single-cell RNA sequencing reveals potential for endothelial-to-mesenchymal transition in tetralogy of fallot. *Congenital Heart Disease* **18(6)**:611–625 DOI 10.32604/chd.2023.047689.